Intermolecular Raman intensity transfer in the v (CO) vibrations of Mn(CO)5Br and Re(CO)5Br

M. Arif and S. F. A. Kettle

Citation: The Journal of Chemical Physics **72**, 2131 (1980); doi: 10.1063/1.439308
View online: http://dx.doi.org/10.1063/1.439308
View Table of Contents: http://scitation.aip.org/content/aip/journal/jcp/72/3?ver=pdfcov
Published by the AIP Publishing

Intermolecular Raman intensity transfer in the ν (CO) vibrations of $Mn(CO)_5Br$ and $Re(CO)_5Br$[a)]

M. Arif and S. F. A. Kettle

School of Chemical Sciences, University of East Anglia, Norwich NR4 7TJ, United Kingdom
(Received 25 October 1978; accepted 21 May 1979)

The change in Raman intensities as (>85%) ^{13}CO enriched $Mn(CO)_5Br$ is isomorphically mixed with $Re(CO)_5Br$ demonstrates that a molecular E mode factor group component steals intensity from a B_1-derived component by an intermolecular process. A mechanism is proposed for this intensity transfer.

The ν(CO) vibrational spectrum of metal pentacarbonyl derivatives of general formulation $M(CO)_5R$ (e.g., $Mn(CO)_5Br$, $Cr(CO)_5P(C_6H_5)_3$) in the 2000 cm^{-1} region have been the subject of many investigations. These compounds have C_{4v} idealized symmetry and so two A_1 ν(CO) spectral features are seen in both infrared and Raman spectra. A further, very strong peak in the infrared spectra of solutions of these compounds is associated with the doubly degenerate E mode. This mode is formally Raman active, but as it correlates with the T_{1u} mode of an octahedral $M(CO)_6$ molecule a very low-intensity is expected. The formally infrared inactive B_1 mode appears strongly in the Raman spectra.[1-10]

In the present communication we are concerned with the appearance of features associated with ν(CO) E modes in the Raman spectrum. Although in solution Raman spectra these E modes have negligible intensity, they are often observed in spectra of crystalline samples where they appear with a wide range of intensities. The range of intensities encountered is shown in Figs. 1–3(a). Figure 1 shows the Raman spectrum of crystalline $Mn(CO)_5I$; any E mode feature would appear at approximately the point marked by X. (This approximate position is determined from the infrared spectrum of a crystalline sample. However, different factor group shifts will occur in infrared and Raman active features.) It is evident that the E mode has little, if any, Raman intensity. An example of weak Raman intensity is provided by $W(CO)_5P(C_6H_5)_3$, the Raman spectrum of which is shown in Fig. 2. Again the E mode is indicated by X. Finally, an intense E mode is shown in Fig. 3(a), where the Raman spectrum of $Mn(CO)_5Br$ is given. The ~2080 cm^{-1} region has, for this compound, been the subject of some discussion.[7-9] The molecular B_1 mode may give rise, at most, to two Raman active factor group components. The appearance of a third strong peak can only be explained by a molecular E mode factor group feature, presumably enhanced by an intensity stealing mechanism. However, this explanation leaves several residual questions. Firstly, which of the three peaks in this spectral region is to be associated with the E mode if a unique assignment is possible? Secondly, why is it that of the four E mode factor group components (A_g, B_{1g}, B_{2g}, and B_{3g} in the $P_{nma}-D_{2h}^{16}$ space group,[7,11a] of which two coincide in symmetry species with the B_1-derived components (B_{1g} and B_{3g}), only one shows any evident intensity stealing? Although the possibility of fortuitous coincidences must not be overlooked it seems most improbable as no splitting is observed on this band for any $M(CO)_5X$ (M = Mn, Re; X = Cl, Br) Raman spectra of either pure or mixed crystal. Further this mode correlates in the molecule with one of the components of the E_g modes of octahedral $M(CO)_6$ species. These E_g modes show extensive factor group splitting so that accidental coincidence would be most surprising. The correlation table appropriate to the present problem is given in Table I.

The general assumption has been that the lowest in frequency of the three features is E mode-derived, a conclusion we definitely establish in this paper.[11b] There has, however, been no discussion of the mechanism of intensity transfer. Two further questions concerning this mechanism arise. Firstly, is the E mode intensity-generating mechanism intra or intermolecular? The absence of E mode Raman activity in the isolated molecule suggests that the latter explanation is appropriate and indeed, we shall shortly demonstrate that the intensity is intermolecular in origin for $Mn(CO)_5Br$. Generalizing this conclusion we are led to the second question. What are the necessary conditions for intermolecular E mode intensification? Three possible conditions are evident to us.

(1) Since an intensity-stealing mechanism is presumably operative, the presence of an intense factor group feature of an identical (factor group) symmetry

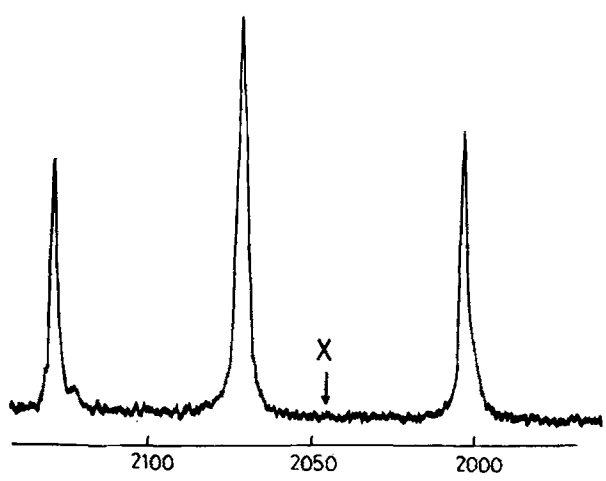

FIG. 1. The Raman spectrum of polycrystalline $Mn(CO)_5I$ in the 2000 cm^{-1} region. The approximate position of any expected molecular E mode feature is indicated by X.

[a)] Solid State Studies. Part 17.

 0021-9606/80/032131-07$01.00

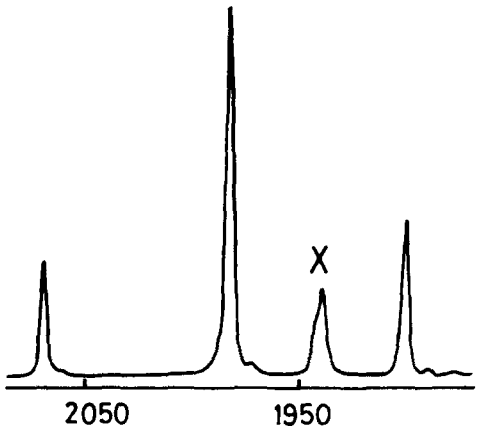

FIG. 2. The Raman spectrum of polycrystalline $W(CO)_5P(C_6H_5)_3$ in the 2000 cm^{-1} region. The feature marked X is derived from the molecular E mode.

species would presumably be necessary.

(2) Similarly, it would be expected from second order perturbation theory that a close frequency correspondence must exist between the two coupled modes if significant intensity transfer is to result.

(3) A proximate packing of the vibrators in the crystal lattice.

In the case of $Mn(CO)_5Br$ condition (1) is assumed to be satisfied; the E mode feature in Fig. 3(a) is presumably of either B_{1g} or B_{3g} factor group symmetry.

The present paper is devoted to a demonstration of the importance of the second of the above conditions. In principle the method to be adopted is simple—one simply has to form a mixed crystal of isomorphous components such that a small frequency difference between relevant modes is replaced by a large frequency separation. This is, indeed, the procedure which we follow, although in practice it proves more difficult than expected. Figure 4 shows the ν(CO) Raman spectrum of $Re(CO)_5Br$. The spectrum of this compound and that of $Mn(CO)_5Br$ are very similar to the 2080 cm^{-1} (ν(CO) B_1 and E mode) region. Not surprisingly, the general appearance of this spectral region is essentially invariant with respect to composition in mixed crystals of the two compounds.[7] The 4 cm^{-1} maximum frequency difference between corresponding features in the spectra of the two pure components is clearly insignificant relative to the magnitude of the intermolecular vibrational coupling.[7]

A rather more drastic perturbation is possible by substituting ^{13}CO for ^{12}CO in $Mn(CO)_5Br$.[7] As ^{13}CO substitution proceeds the bands in the 2080 cm^{-1} region broaden and disappear to be replaced by similar bands

TABLE I. Correlations between molecular, site, and factor groups.

Molecular Point Group C_{4v}	Site Group C_s	Factor Group D_{2h}^{16}, $z=4$
A_1 (IR R)	A' (IR R)	A_g (R)
B_2 (R)		B_{2g} (R)
E (IR R)		B_{1u} (IR)
		B_{3u} (IR)
B_1 (R)	A'' (IR R)	B_{1g} (R)
A_2 –		B_{3g} (R)
		A_u –
		B_{2u} (IR)

IR – infrared R = Raman

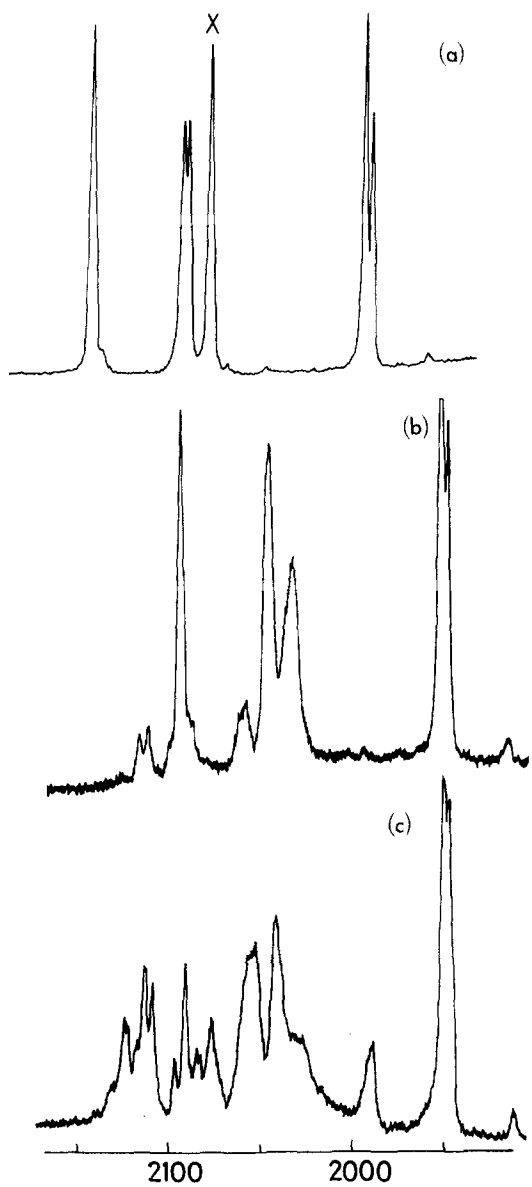

FIG. 3. (a) The Raman spectrum of polycrystalline $Mn(CO)_5Br$ in the 2000 cm^{-1} region. The feature marked X is derived from the molecular E mode. (b) The Raman spectra of ^{13}CO-enriched (> 85%) polycrystalline $Mn(CO)_5Br$ in the 2000 cm^{-1} region. (c) The Raman spectra of ^{13}CO-enriched (~ 60%) polycrystalline $Mn(CO)_5Br$ in the 2000 cm^{-1} region.

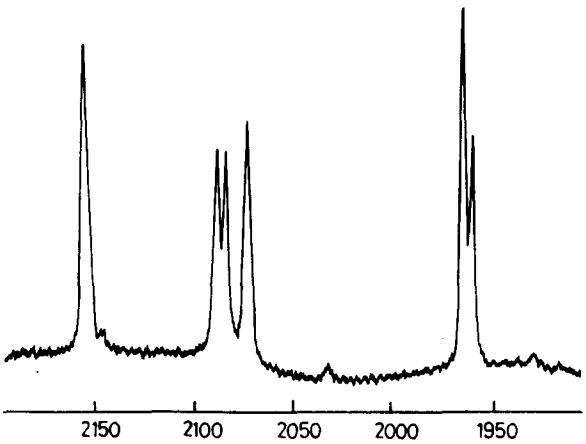

FIG. 4. The Raman spectra of polycrystalline $Re(CO)_5Br$ in the 2000 cm^{-1} region.

in the 2035 cm^{-1} region. The Raman spectrum of a sample with a high level of ^{13}CO substitution is shown in Fig. 3(b) and one with a lower level in Fig. 3(c). As the bands in the 2080 cm^{-1} region weaken, the low frequency band remains the most intense and indeed, probably increases in intensity; of those in the 2035 cm^{-1} [molecular axial ν(CO) region], the low frequency band appears to be the weaker. Clearly, the perturbations arising from ^{13}CO substitution, although affecting the intensity of the low frequency band, do so in a rather complicated way. In mixed crystals containing, say, 50% of ^{13}CO there will be ten different molecular species present in significant quantity resulting in a total of eighteen different site occupancies. Simple behavior is not to be expected and we do not attempt a detailed interpretation in the present paper.[7]

When intermolecular vibrational coupling occurs one is no longer concerned with the vibrations of individual molecules. The question of the consequent vibrational effects of replacing molecules with isotopic variants has been extensively studied by the present authors. It is clear[7] that intermolecular vibrational coupling is important in the 2080 cm^{-1} region for $Mn(CO)_5Br$; the peak broadening on ^{13}CO substitution implies that the isotopic species present maintain coupling with the nonisotopic host (this is the so-called intermediate mode behavior[7]). Similar considerations apply to isotopic variants of $Mn(^{13}CO)_5Br$, thus, intermediate mode behavior means that the 2043 cm^{-1} peak in Fig. 3(b) does not show the splitting of the corresponding 2090 cm^{-1} peak in Fig. 3(a). Because of this coupling in the 2020–2050 cm^{-1} region of Fig. 3(b) we shall for simplicity call the species of Fig. 3(b) $Mn(^{13}CO)_5Br$. For the same reason, that of coupling between and therefore of an averaging over isotopic variants, we shall for this spectral region take Table I to be applicable, notwithstanding the fact that some isotopic variants will not have molecular C_{4v} symmetry.

Although in a molecular B_1 mode the metal atom does not move, it does participate in molecular E modes. Substitution by ^{13}CO in $Mn(CO)_5Br$ will have a relatively small effect on this participation. Much more significant would be replacement of Mn by Re. This recognition, together with the frequency shifts provided by ^{13}CO substitution in $Mn(CO)_5Br$, led us to what proved to be the key experiment; the study of the Raman spectra of a series of mixed crystals containing $Re(CO)_5Br$ and $Mn(^{13}CO)_5Br$ in various proportions. In these studies, the sample of $Mn(^{13}CO)_5Br$ used was that of the spectrum shown in Fig. 3(b).

Figures 5(a)–(c) show the Raman spectra of mixed crystals of general composition $[Mn(^{13}CO)_5Br]_x \times [Re(CO)_5Br]_{1-x}$ for $x \simeq 0.25$ [Fig. 5(a)], $x \simeq 0.47$ [Fig. 5(b)] and $x \simeq 0.59$ [Fig. 5(c)]. Figures 4 and 3(b) may also be considered to be in this series with $x = 0$ and $x = 1$, respectively. Frequencies are detailed in Table II. Particularly striking in this series is the almost complete disppearance of the E mode derived feature of $Re(CO)_5Br$ in Fig. 5(c). Unfortunately, it is not possible to comment with certainty on whether the lost

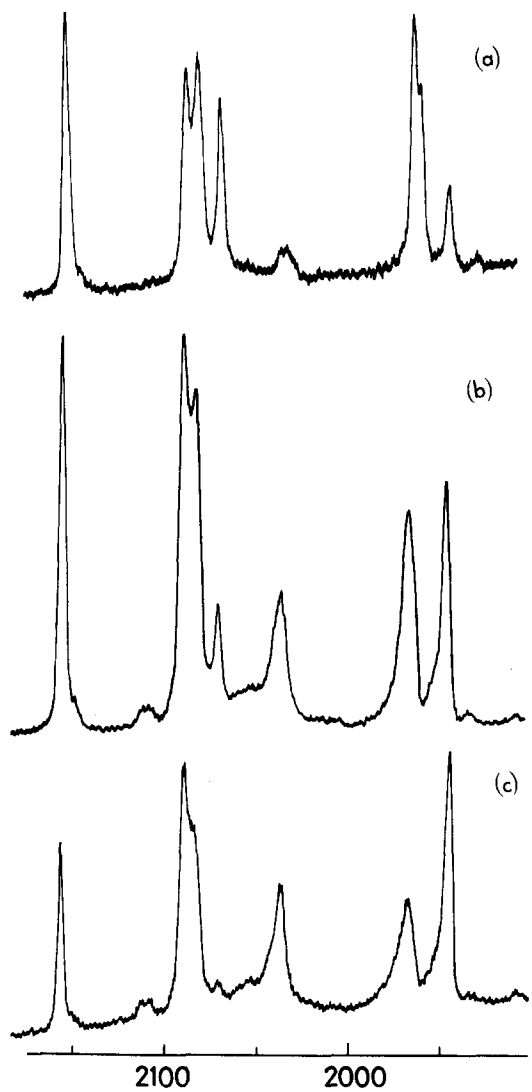

FIG. 5. (a) The Raman spectrum of polycrystalline $[Mn(^{13}CO)_5Br]_x[Re(CO)_5Br]_{1-x}$ in the 2000 cm^{-1} region. ($x \simeq 0.25$). (b) The Raman spectrum of polycrystalline $[Mn(^{13}CO)_5Br]_x[Re(CO)_5Br]_{1-x}$ in the 2000 cm^{-1} region. ($x \simeq 0.47$). (c) The Raman spectrum of polycrystalline $[Mn(^{13}CO)_5Br]_x[Re(CO)_5Br]_{1-x}$ in the 2000 cm^{-1} region. ($x \simeq 0.59$).

TABLE II. Solid Raman frequencies (cm^{-1}) of mixed crystals of ^{13}Co-enriched $Mn(CO)_5Br$ and $Re(CO)_5Br$ in the $\nu(CO)$ region.

		Pure $Re(CO)_5Br$	Enriched $Mn(CO)_5Br$	Mixed crystal of enriched $Mn_x(CO)_5Br$ & pure $Re_{1-x}(CO)_5Br$ $x=0.59$ $1-x=0.41$	$x=0.47$ $1-x=0.53$	$x=0.25$ $1-x=0.75$
	A_1	2155	2092[a]	2157	2157	2156
		2089		2090	2090	2090
Re	B_1	2083		2084	2084	2084
Re	E	2071		2071	2071	2072
Mn	B_1 & E		2043 2029	2036 2038	2037	2040 2035
Re	A_1	1964 1960		1968	1967	1965 1962
Mn	A_1		1948 1944	1944	1946	1947

intensity reappears in one of the molecular B_1-derived features because of the coincidence between the higher of them and the $Mn(^{13}CO)_5Br$ equatorial A_1 peak. Just as in the mixed crystal, the rhenium E mode peak disappears, so too, in Fig. 5(c), the ^{13}CO B_1 features of $Mn(^{13}CO)_5Br$ appear as a single peak; that is, there is no E-derived component there either. This should be compared with Fig. 3(b) where $Mn(^{13}CO)_5Br$ shows two peaks in this region.

Four main conclusions emerge from these observations. Firstly, as has been generally supposed, the low frequency band in the 2080 cm^{-1} region of $Mn(CO)_5Br$ is an E mode factor group component, made visible by coupling with a B_1-derived mode of the same species. The possibility that the E mode intensity arises from crystal lattice distortion effects may also be dismissed. Because the intensity persists in $[Mn(^{12}CO)_5Br]_x \times [Re(^{12}CO)_5Br]_{1-x}$ mixed crystals[7] but disappears as $Mn(^{12}CO)_5Br$ is replaced by $Mn(^{13}CO)_5Br$ a lattice explanation is untenable. Secondly, the mechanism for intensity transfer is, likewise, intermolecular in origin. Thirdly, as noted above, as the concentration of $Re(CO)_5Br$ decreases the $\nu(CO)$ B_1 peak of this compound is replaced—at an almost identical frequency—by the $\nu(^{13}CO)$ A_1 equatorial peak of $Mn(^{13}CO)_5Br$. These two modes differ in their behavior under reflection in the crystallographic mirror plane. The latter is symmetric and the former is antisymmetric. It follows that they subtend no common factor group symmetry species. The loss of intensity from the $\nu(CO)$ E mode feature of $Re(CO)_5Br$ clearly demonstrates that it is not sufficient for there to be a mode at the correct frequency for intensity stealing to occur; it also has to be of the correct symmetry. Fourthly, the intensity stealing mechanism is not a simple "through space" coupling. Since the coupling is sensitive to G-matrix changes a mechanism involving proximate molecules is implicated.

TABLE III. Frequencies (cm^{-1}) of $\nu(CO)$ B_1 and E modes for some $M(CO)_5X$ species.

Species	B_1	E
$Mn(CO)_5Br$	2080[a]	2053[b]
$Re(CO)_5Br$	2080[c]	2046[b]
$Mn(CO)_5I$	2072[a]	2046[b]
$W(CO)_5P(C_6H_5)_3$	1981[a,b]	1941[b]

[a]Observed in the solution Raman spectrum.
[b]Observed in the solution infrared spectrum.
[c]Calculated value.

TABLE IV. The major spectral features associated with the $\nu(CO)$ B and E modes of IR and Raman spectra of some crystalline $M(CO)_5X$ species.

	$Mn(CO)_5Cl$		$Re(CO)_5Cl$		$Mn(CO)_5Br$	
Mode	IR	R	IR	R	IR	R
B_1	2085 m	2095 vs	2080 m	2091 ms 2088 sh	2084 m	2090 ms 2087 ms
E	2073 s 2060 sh 2050 vs	2079 s	2062 s 2039 vs	2074 s	2070 s 2050 vs	2075 s
	$Re(CO)_5Br$		$Mn(CO)_5I$		$Re(CO)_5I$	
B_1	2081 m	2089 s 2083 s		2072 s		2073 s
E	2063 s 2053 sh 2040 s	2071 s	2055 sh 2045 s 2037 sh		2055 sh 2035 vs 2007 sh	
	$Cr(CO)_5P(C_6H_5)_3$		$Mo(CO)_5P(C_6H_5)_3$		$W(CO)_5P(C_6H_5)_3$	
B_1	1994 sh 1991 s	1989 vs	1997 ms 1982 sh	1990 vs	1986 ms 1970 sh	1982 vs
E	1945 s 1930 s	1945 sh 1941 ms	1950 s 1937 s	1949 sh 1946 m	1943 s 1930 s	1941 sh 1938 m

[a]The Mn (A_1) mode overlaps with the B_1 (Re) band in the mixed crystal spectra.

There are two aspects to this, the relationship between molecular vibrational frequencies and the spatial relationship between molecular vibrators. The former is detailed in Table III, which compares $\nu(CO)$ B_1 and E mode features for the four species discussed in this paper as observed in solution and Table IV which gives some corresponding data for crystalline samples.

It is clear from Table III, that the occurrence of a strong E mode feature is not immediately related to the frequencies of the isolated molecule. Thus, the separation between the B_1 and E frequencies are essentially identical for $Mn(CO)_5Br$ and $Mn(CO)_5I$, yet, as seen from Figs. 1 and 3(a), the bromide has a strong Raman active E mode feature whilst for the iodide there appears to be no such feature. In Table IV, the first four isomorphous[11a] compounds all have strongly Raman active E modes whereas the E-derived features are significantly weaker for the three isomorphous phosphine derivatives and very weak for the two iodides. It is clear that, although a frequency comparability of B_1 and E modes is presumably a necessary precondition for intensity transfer to occur, it is the crystal structure which determines whether significant coupling occurs. That is, a correct spatial relationship must exist be-

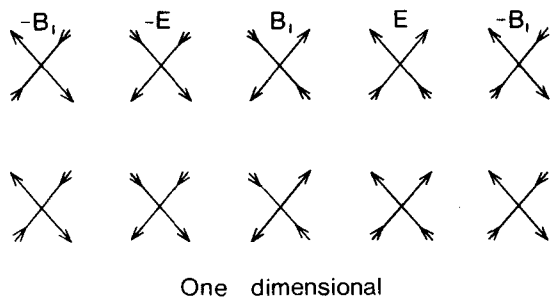

FIG. 6. Postulated "one dimensional" coupling between molecular B_1 and E vibrators.

tween the molecules in the crystal lattice. Further, the crystal structure adopted by the $M(CO)_5X$ species where M = Mn, Re and X = Cl, Br must presumably be close to the optimum.

Before considering this crystal structure in detail it is convenient to postulate and to distinguish two coupling mechanisms, which by virtue of their different two-dimensional projections, we may conveniently call one-dimensional and two-dimensional couplings. These mechanisms are schematically shown in Figs. 6 and 7. It is to be noted that these two mechanisms are not mutually exclusive. The common feature of these mechanisms is a coupling between local dipolar components of B_1 and E modes. Two points should be made. Firstly, although it is convenient to talk of and to symbolize a simple dipolar coupling as we have pointed out, it is clear from the experimental evidence that the coupling is not simply "through space" but that a mechanical mechanism is also implicated. Secondly, in the case of ~50% ^{13}CO substituted $Mn(CO)_5Br$, for which a considerable number of isotopic site arrangements exist, the number of local isotopic site *patterns* analogous to those of Figs. 6 and 7, will be very large indeed. It is therefore understandable that such a complicated Raman spectrum should be obtained for such a level of isotopic substitution, since the features observed will be dependent on both the statistics of the many arrangements and the way that phase coherence decays with distance for each.

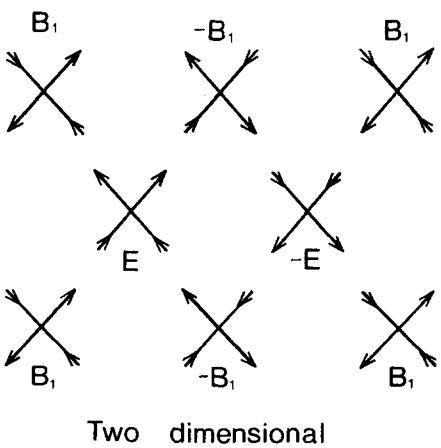

FIG. 7. Postulated "two dimensional" coupling between molecular B_1 and E vibrators.

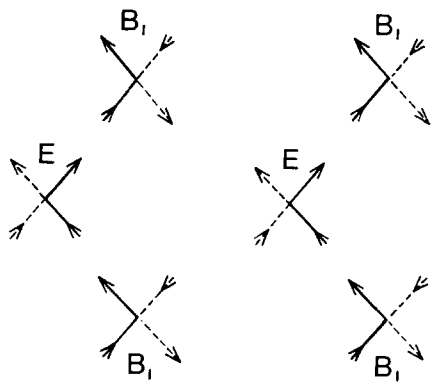

FIG. 8. Coupling of totally symmetric factor group components of molecular B_1 and E vibrators.

Consideration of Figs. 6 and 7 leads to a generalization concerning the mechanisms shown there, a generalization which, however, has to be subject to an exception which we shall discuss shortly. This generalization is that, "Significant intensity transfer between molecular-symmetry distinct vibrations will usually only occur between vibrations which are nontotally symmetric in the factor group."

The origin of this generalization is simple. When vibrations of different molecular symmetries are coupled, vibrator phase-matching of the type shown in Figs. 6 and 7 will only occur for factor group combinations which are antisymmetric with respect to some operations. These combinations cannot, therefore, be totally symmetric in the factor group. An exception to this rule which is evident to us will be when some of the vibrators are buried in an insulating (nonvibrationally coupled) environment, as may occur in low-symmetry unit cells such as $P\bar{1}$, where all Raman-allowed vibrations must be totally symmetric. An illustration of this situation is given in Fig. 8, where the "insulated" vibrators are shown dotted.

Of the two mechanisms which we postulate, that appropriate to $Mn(CO)_5Br$ and its isomorphs is the two-dimensional case for the factor group B_{1g} mode. In Fig. 9 we show the molecular B_1- and E-derived factor group components and in Fig. 10 indicate the way that they may couple. The relevant oxygen–oxygen interatomic separations are shown in Fig. 11, from which it is seen that the oxygen atoms of CO vibrators required to couple in the proposed mechanism are all less than 3.5 Å apart. The intermolecular coupling between molecular B_1 and E modes has the effect of mixing to-

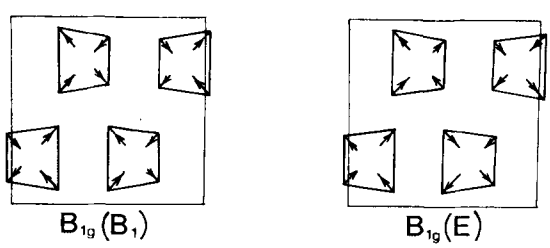

FIG. 9. The B_{1g} factor group derivatives of molecular B_1 and E modes in crystalline $Mn(CO)_5Br$.

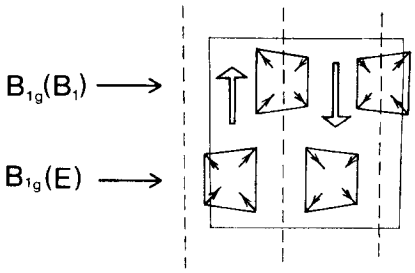

FIG. 10. The "two dimensional" coupling mechanism for molecular B_1 and E modes in crystalline $Mn(CO)_5Br$.

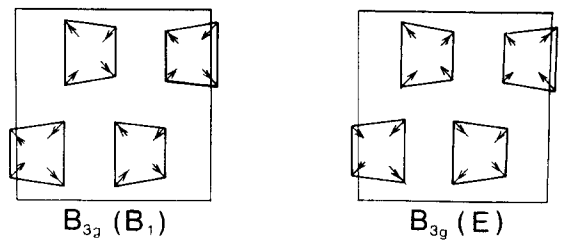

FIG. 12. The B_{3g} factor group derivatives of molecular B_1 and E modes in crystalline $Mn(CO)_5Br$.

gether these modes within an individual molecule. It is easy to show that the resulting molecular modes have the form shown in Fig. 8, where the dotted internal coordinates are those that make but a small contribution to the coupled B_1–E mode shown. Finally, it is not difficult to see that no analogous extended coupling mechanism exists in the case of the common B_{3g} B_1- and E-derived factor group modes. This is illustrated in Fig. 12 which shows the two B_{3g} modes. It is clear from the diagrams that there is no possible head-to-tail matching of dipoles and consequently, no effective mechanism for intermolecular coupling. This distinction between the B_{1g} and B_{4g} modes suggests that a coupling mechanism analogous to that which we have invoked for the former may be responsible for the strong factor group coupling sometimes observed in features derived from molecular modes which do not subtend a dipole (although here only a single molecular mode would be involved). Thus, in the case of $M(CO)_5X$ species, the presence of factor group coupling on molecular B_1 modes may perhaps be associated with local *intermolecular* dipoles (as seen in Fig. 10) compared with the intramolecular dipoles of the E modes (implied in Fig. 10). The B_1–E coupling mechanism which we have invoked is essentially, a coupling of a B_1-derived intermolecular dipole with an E-derived intramolecular dipole. This approach makes the distinction between the B_{1g} and B_{3g} factor group cases clear. In the latter there is no B_1-derived intermolecular dipole (Fig. 12).

The compounds $M(CO)_5P(C_6H_5)_3$ M = W, Mo are both isomorphous to the corresponding chromium compound, the structure of which has been determined by Plastas, Stewart, and Grim.[12] The centrosymmetric nature of the unit cell ensures that some CO groups are proximate but the large triphenylphosphine ligand undoubtedly acts as an insulation and reduces the extent of the coupling which occurs. For this molecule a coupling mechanism such as that indicated in Fig. 8 might be appropriate since in $P\bar{1}$ all Raman-active modes must be totally symmetric. Whilst this may not be totally untrue, the crystal structure is such that our one-dimensional mechanism seems more relevant to the observation of some Raman intensity in the ν(CO) E mode-derived factors. However, it has yet to be conclusively established for these compounds that the E mode intensity is intermolecular in origin and so further speculation is premature.

a = 3·30
b = 3·30
c = 3·46
d = 3·41
e = 3·19
f = 3·37

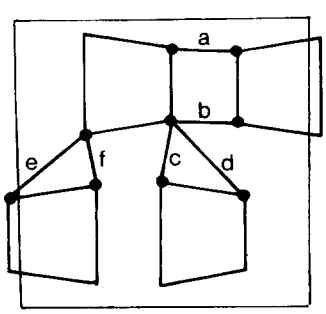

FIG. 11. Oxygen–oxygen separations in crystalline $Mn(CO)_5Br$.

CONCLUSION

The present study has shown the potential danger of a facile interpretation of Raman intensities in the spectra of crystalline solids. An experimental approach to a detailed understanding has been described and a qualitative model of coupling mechanisms appropriate to the cases under study has been presented.

EXPERIMENTAL

All compounds were prepared by standard procedures.[13–15] The ^{13}CO exchange reactions were carried out with 100 mg of $Mn(CO)_5Br$ in 100 ml hexane using ^{13}CO (97.4% Prochem). Each exchange reaction was carried out in the dark at 50° for five days. Mixed crystals were prepared by rapidly cocrystallizing at −78° weighted amounts of each component. Acetone was used as solvent. The resulting crystals were dried under vacuum.

Exchange of CO between gaseous (or dissolved) CO and $Mn(CO)_5Br$ is known to be relatively slow; that with $Re(CO)_5Br$ is even slower. Any significant CO exchange between $Mn(^{13}CO)_5Br$ and $Re(CO)_5Br$ on cocrystallization is therefore most improbable. That none has occurred is confirmed by a comparison of the highest frequency ν(CO) Raman active bands in the pure and mixed crystals. These bands are associated with two-mode behavior and so are molecule localized; intermolecular effects do not affect the band patterns. Thus, the two small isotopic highest frequency bands seen in Fig. 3(a) are also seen with appropriate intensity in Figs. 5(a), 5(b), and 5(c). It was on the basis of the relative intensities of these bands, the signal-to-noise ratio and a pessimistic approach to the assumption of band intensity invariance to isotopic substitution that a lower limit of enrichment was obtained for the most ^{13}CO-enriched sample of $Mn(CO)_5Br$.

Raman spectra were recorded at room temperature using a Spex 1401 monochromator with photon counting. A Spectra Physics 165 Ar/K laser operating at 6471 Å was used, the power incident on the sample being ~20 mW. A scanning speed of 5 cm^{-1} min^{-1} was maintained with a resolution of 2 cm^{-1}.

ACKNOWLEDGMENT

One of us (MA) is indebted to the Ministry of High Education, Iraq for financial support. The support of the Royal Society is also acknowledged.

[1]T. A. Magee, C. N. Matthews, T. S. Wang, and J. H. Wotiz, J. Am. Chem. Soc. 83, 3200 (1961).
[2]L. E. Orgel, Inorg. Chem. 1, 75 (1962).
[3]F. A. Cotton, A. Musco, and G. Yagupsky, Inorg. Chem. 6, 1357 (1967).
[4]H. D. Kaesz, R. Bau, D. H. Hendrickson, and J. M. Smith, J. Am. Chem. Soc. 89, 2844 (1967).
[5]I. S. Butler and H. K. Spendjian, Can. J. Chem. 47, 4117 (1969).
[6]I. J. Hyams and E. R. Lippincott, Spectrochim. Acta Part A 25, 1845 (1969).
[7]D. Kariuka and S. F. A. Kettle, Spectrochim. Acta Part A 34, 563 (1978).
[8]R. J. H. Clark and B. C. Crosse, J. Chem. Soc. A 224 (1969).
[9]E. W. Abel and G. Wilkinson, J. Chem. Soc. 1501 (1959).
[10]D. K. Ottesen, H. B. Gray, L. H. Jones, and M. Goldblatt, Inorg. Chem. 12, 1051 (1973). This paper reports solution Raman spectra in the 2000 cm^{-1} region, and gives infrared and lower frequency Raman data for normal and isotopic species together with an excellent vibrational analysis.
[11](a) P. J. Greene and R. F. Bryan, J. Chem. Soc. A 1559 (1971); (b) In that the lower frequency peak appears to be the more intense some effective "crossing over" of B_1 and E-derived features probably occurs. It is this peak which is sensitive to the isotopic dilution technique used in this work and so unscrambles in correlation with the E-derived peak.
[12]H. J. Plastas, J. M. Stewart, and S. O. Grim, Inorg. Chem. 12, 265 (1973).
[13]*Organometallic Synthesis*, edited by J. J. Eisch and R. B. King (Academic, New York, 1965), Vol. 1.
[14]E. W. Abel and G. Wilkinson, J. Chem. Soc. 1501 (1959).
[15]G. B. Blakney and G. F. Allen, Inorg. Chem. 10, 2763 (1971).